A Structural Perspective on the Dynamics of Kinesin Motors

Changbong Hyeon[†*] and José N. Onuchic[‡*]
[†]School of Computational Sciences, Korea Institute for Advanced Study, Seoul, Republic of Korea; and [‡]Center for Theoretical Biological Physics, Rice University, Houston Texas

ABSTRACT   Despite significant fluctuation under thermal noise, biological machines in cells perform their tasks with exquisite precision. Using molecular simulation of a coarse-grained model and theoretical arguments, we envisaged how kinesin, a prototype of biological machines, generates force and regulates its dynamics to sustain persistent motor action. A structure-based model, which can be versatile in adapting its structure to external stresses while maintaining its native fold, was employed to account for several features of kinesin dynamics along the biochemical cycle. This analysis complements our current understandings of kinesin dynamics and connections to experiments. We propose a thermodynamic cycle for kinesin that emphasizes the mechanical and regulatory role of the neck linker and clarify issues related to the motor directionality, and the difference between the external stalling force and the internal tension responsible for the head-head coordination. The comparison between the thermodynamic cycle of kinesin and macroscopic heat engines highlights the importance of structural change as the source of work production in biomolecular machines.

INTRODUCTION

In recent years, technological advances have revolutionized our understanding of biological systems by providing unprecedented views of biomolecular dynamics at the single molecule level, bringing into reality what Feynman envisioned on nanotechnology 50 years ago (1). The scenery inside the cell unveiled by nanodevices displays beautiful tempo-spatial organization. Among a host of macromolecules that constitute the cell, of particular interest are specialized enzymes, namely biological motors that convert chemical energy stored in substrate molecules into mechanical work (2). From transport motors that move along cytoskeletal filaments (kinesin, dynein, myosin) (3,4) to the sophisticated protein production machinery (ribosome) (5,6), biological motors play vital roles in controlling cellular functions, such as gene expression, intra- and intercellular trafficking, cell motility, and mitosis (7). A malfunction in these motors can cause detrimental effects in the cell. In the highly dissipative nanoscale environment that immediately randomizes any ballistic motion, it is amazing to see how these evolutionarily tailored molecules carry out biological functions with exquisite precision. Elucidating physical principles that bring molecular machines into action is one of the most challenging problems in modern biology.

Despite notable progress made in current nanotechnology, a precise vision on biological motors still remains elusive due to ineluctable thermal noise in nanoscopic measurements. The questions begged from experiments demand additional details of the structures and dynamics of molecules (8,9), which require greater spatial, temporal resolutions and better control than current techniques can provide

(10). To this end, simulations using molecular models of biological motors (11–18) can supplement the current experimental findings and make insightful predictions amenable to future experimental investigations.

In the study of biological motors, however, computational approach using molecular simulations has been relatively rare compared with other areas focusing on folding dynamics of small-sized proteins. This is partly because the typical size and timescale associated with biological motors are far greater than usual computational approaches have dealt with. Nevertheless, biomolecular dynamics have a hierarchical structure in terms of their timescale, characterized with a large timescale separation between atom (~fs), residues (~ps), and domain motions ($\gtrsim \mu s - $ ms). To study the dynamics associated with a particular range of timescale, faster degrees of freedom can be renormalized into an effective degree of freedom. As long as the topological feature characterizing molecular structures are unchanged, coarse-graining the atomistic details does not essentially alter the global motion responsible for biological function. Thus, the biology can employ the strategy of condensed matter physics that simplifies the phenomenon of interest based on its timescale, and relevant degrees of freedom (19,20) can be applied to the biology. Together with the current technical advances in single molecule measurements on diverse biological motor systems, dynamics generated from coarse-grained representation of motors allow one to grasp the gist of design principle under which each biological motor performs its biological function. In this perspective, recent efforts made in studying the dynamics of various biological motors using coarse-grained models (11–18) are quite promising.

Physical conditions that govern the dynamics of objects in the nanoscopic to microscopic world are fundamentally different from those for the macroscopic objects (see

Supporting Material) text and Fig. S1 in the Supporting Material). To this end, the conceptual framework developed from the theory of protein folding (21–24) and polymer physics (25), which handle the complex dynamics of chain molecules over multiscale, is of great use to decipher the design principles of biological motors. Here, we will discuss the dynamics of kinesin by comparing our insight gained from a structure-based coarse-grained model of kinesin with the experimental findings in each stage of the biochemical cycle. Finally, we will construct a thermodynamic cycle of kinesin using the neck linker (NL), a key mechanical element responsible for work generation, and highlight the importance of structural change in producing net mechanical work per cycle and in the regulation.

GENERAL OVERVIEW: BIOCHEMICAL STATES OF KINESIN

Kinesin-1 (hereafter kinesin) transports cellular organelles along the network of cytoskeletal filaments and plays a central role in spatially organizing the cellular environment. Two identical motor domains, linked via coiled-coil stalk, alternately exploit the free energy generated from ATP molecules to produce characteristic 8-nm steps. Single molecule experiments have revealed that at the physiological condition, kinesins can processively travel ~100 steps in a hand-over-hand fashion at a velocity of $v \approx 1 \ \mu m / s$ (26–28).

Recently, a growing number of kinesin structures, with various ligand states, have shed light on more detailed mechanisms of how kinesins function. A series of crystal structures suggest how kinesins adapt their conformation to varying nucleotide (NT) states via $\rightarrow [\phi \rightarrow ATP \rightarrow ADP \cdot Pi \rightarrow ADP] \rightarrow$ (Fig. S2). It is currently surmised that the local conformational changes due to the NT chemistry are amplified via the switch II helix (α4) to regulate i), the NL conformation and ii), the binding affinity to microtubules (MTs) (29). For kinesin-1, the states of NL and MT affinity are the two major components that determine the logic of biochemical cycle. Depending on the NT state, the NL is in either ordered (zippered) or disordered (unzippered) state; the binding affinity of kinesin head domain to MTs is either strong or weak. The relationship between these two binary switches in a single head, summarized in Table 1 (see also Fig. S2, b and c), forms a basic logic for the kinesin dynamics.

The four different NT states (ϕ, ATP, ADP·Pi, ADP) at the catalytic site enable one to assign, in principle, 16 different states to the kinesin dimer; however, most of the possible dimer states has to be excluded. First, the ADP-ADP state (the notation $(NT)_L$-$(NT)_R$ represents the NT state of trailing and leading head from left to right and we assume kinesins move from left (– end) to right (+ end). Below, we omit $(\cdots)_L - (\cdots)_R$ in the notations), corresponding to the weak-weak MT binding state, should be excluded because at least one of the heads should hold MTs tightly to remain on the MT track. Second, due to the topological constraint imposed by the NL zipper in the leading head (Fig. S2 c), the NL of the leading head cannot be in an ordered state, which prohibits the ϕ-ATP, ATP-ATP, and ADP-ATP (or ϕ-ADP·Pi, ATP-ADP·Pi, and ADP-ADP·Pi) states from the possible dimer states. ϕ-ADP and ϕ-ϕ states are also unlikely to exist because the time spent for ATP to dissociate from the trailing head (ATP → ADP·Pi → ADP → ϕ) (> 1 s (30)) is longer than the time-scale associated with ADP dissociation from the leading head ($\lesssim 10$ ms (30)). Therefore, only four states (ATP-ADP, ATP-ϕ, ADP·Pi-ϕ, and ADP-ϕ) are permissible out of the 16 states. The conventionally accepted kinesin cycle is schematized in Fig. 1 (31–33).

To sustain a constant material flux along the biochemical cycle, kinesins need a continuous supply of ATP (source) and removal of ADP and Pi (sink) (see Supporting Material text for the discussion on nonequilibrium steady-state thermodynamics). In the kinesin cycle depicted in Fig. 1, ATP binding induced stepping ($[ADP-\phi]_{i-1} \rightarrow [ATP-ADP]_i$) is the only mechanical motion (*yellow arrows* in Fig. 1) that can be detected with single molecule measurements (*inset* of Fig. 1). All other steps (*purple arrows* in Fig. 1) are associated with internal chemistry. In contrast to the common notion for macroscopic heat engines where heat released from combustion is directly used to expand the volume of cylinder and provide the power stroke (see Fig. S1 and Supporting Material text), the heat released from the ATP hydrolysis step in the catalytic site itself is not the main driving force of the stepping motion. A series of structures that vary with NT state and biochemical data indicate that the ATP hydrolysis itself alters neither the NL state nor the affinity to MT. For kinesins, the free energy released from the ATP hydrolysis at the catalytic site is estimated to be relatively small $\approx 4 \ k_B T$ (34–36). Even though the free energy change due to ATP hydrolysis in the catalytic site is small, the irreversibility of the enzymatic cycle set by the ATP hydrolysis has an important implication for the robust action of biological motors (37).

ATP BINDING-INDUCED CONFORMATIONAL CHANGE

ATP binding to a catalytic site creates new contacts to the residues that constitute the catalytic site ($\Delta H < 0$), and reduces the local fluctuations ($\Delta S < 0$). As long as the stabilization free energy ($\Delta G = \Delta H - T\Delta S$) remains negative, the ATP binding is favored. Previously, using the molecular

TABLE 1   NT state-dependent configuration of a kinesin monomer

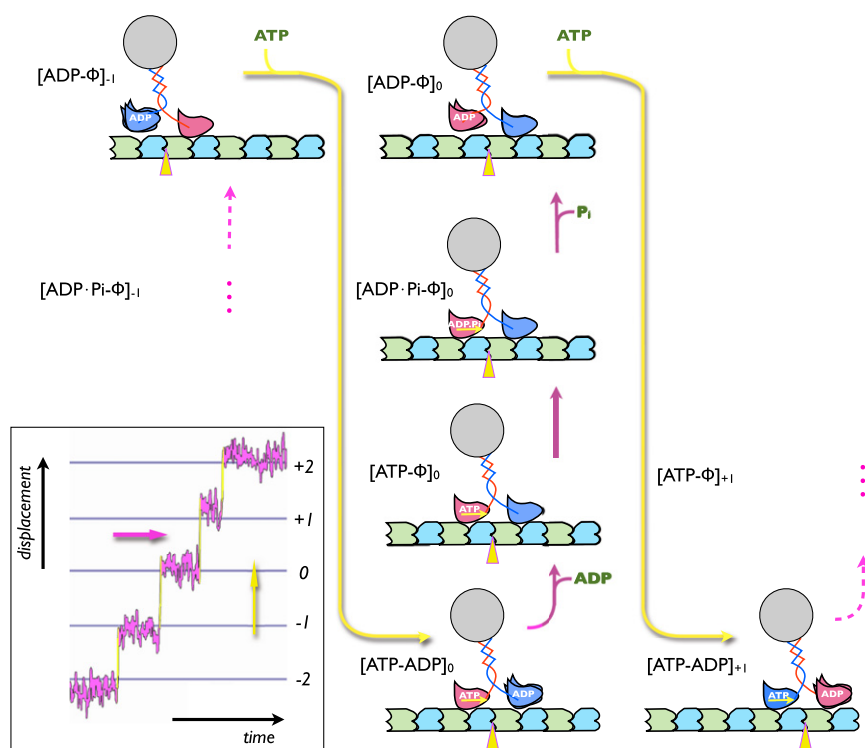|	NL state (40)	Affinity to MTs (31)
$K \cdot \phi$	Disordered (off)	Strong ($K_d \sim$ nM)
$K \cdot$ATP	Ordered (on)	Strong
$K \cdot ADP \cdot$Pi	Ordered (on)	Strong
$K \cdot$ADP	Disordered (off)	Weak ($K_d \sim \mu$M))

FIGURE 1 Biochemical cycle of a kinesin motor. The state of kinesin changes along the cycle. The subscript i in the notation $[NT\text{-}NT]_i$ denotes the position on MT to which the kinesin binds. In the diagram the internal conformational states that do not alter the kinesin position are aligned vertically with purple arrows, and the step is depicted with yellow arrows. The inset shows a time trace from laser optical tweezers measurement.

simulation we have shown for the catalytic domain of protein kinase A that local compaction of ligand binding pocket upon ATP binding induces a global open-to-closed transition (38). For kinesin, despite the presence of a number of high-resolution cryo-electron microscopy or crystal structure data (29,39), it is still an open question how explicitly the intramolecular signal transduction leads to the disorder-order transition in the NL. Nevertheless, the difference in the contact maps before and after the formation of NL zipper (Fig. 2 a) can be used to calculate the folding landscape of kinesin for each case. From the perspective of energy landscape, visualized in terms of the centroid of tethered head whose motion is constrained by the NL (see Fig. 2 b) (14), it could be argued that ATP binding reshapes the energy landscape from the disordered state ($F_{disorder}(\{\vec{r}\})$) to the ordered state ($F_{order}(\{\vec{r}\})$), and gives rise to a conformational force ($\vec{f}_{conf}(\{\vec{r}\}) = -\vec{\nabla} F(\{\vec{r}\})$), which can be interpreted as the power stroke. The NL zipper formed in the MT-bound head biases the diffusive motion of the tethered head toward the (+)-end direction, which has also been termed the NL docking model (40).

One well-known objection to the NL docking model as a driving force for the kinesin step is that the free energy gain calculated from electron paramagnetic resonance measurement $\Delta G_{dock} \approx -1.2\ k_B T$ (9,41,42), is energetically insufficient to drive the kinesin step. However, as will be discussed in the next section, the energetic contribution of the NL docking (or power stroke) to the stepping motion

needs not necessarily be large as long as the NL zippered state can provide enough anisotropic bias, so that the tethered head can reach the next MT binding site through the diffusive search. Interestingly, recent single molecule experiments and computation have suggested that a structural motif called cover-neck bundle (see Fig. 2 a) can guide the early stage of the NL docking dynamics (43,44). In addition, a simple back-of-envelope calculation using available thermodynamic/kinetic data provides a much greater estimate of the net stability difference involving the step from $[ADP\text{-}\phi]_{i-1}$ to $[ATP\text{-}ADP]_i$ as $\Delta G_{step} \approx (-10\ \sim\ -12)\ k_B T$ (35,36,45) for quasistatic processes, which agrees with the work required to stall the kinesin motion $W = (6-7)$ pN $\times$ 8 nm $\approx 12\ k_B T$. ΔG_{step}. This is expected to consist of ΔG_{dock} and other free energy contributions due to the interaction between the ADP containing tethered kinesin head and MT surface. In fact, how tightly or loosely the free energy of molecular fuel is coupled to the functional motion is the key question that has been asked for many different motors (46). Similarly, contrasting the mechanism of power stroke (or conformational change) with Brownian ratchet (or diffusive motion) may be a useful way to dissect the role of energetics and flexibility of molecular machines in performing their functional motion.

STEPPING DYNAMICS

The stepping motion in search of the next MT binding site is the most dramatic and functionally important step in the
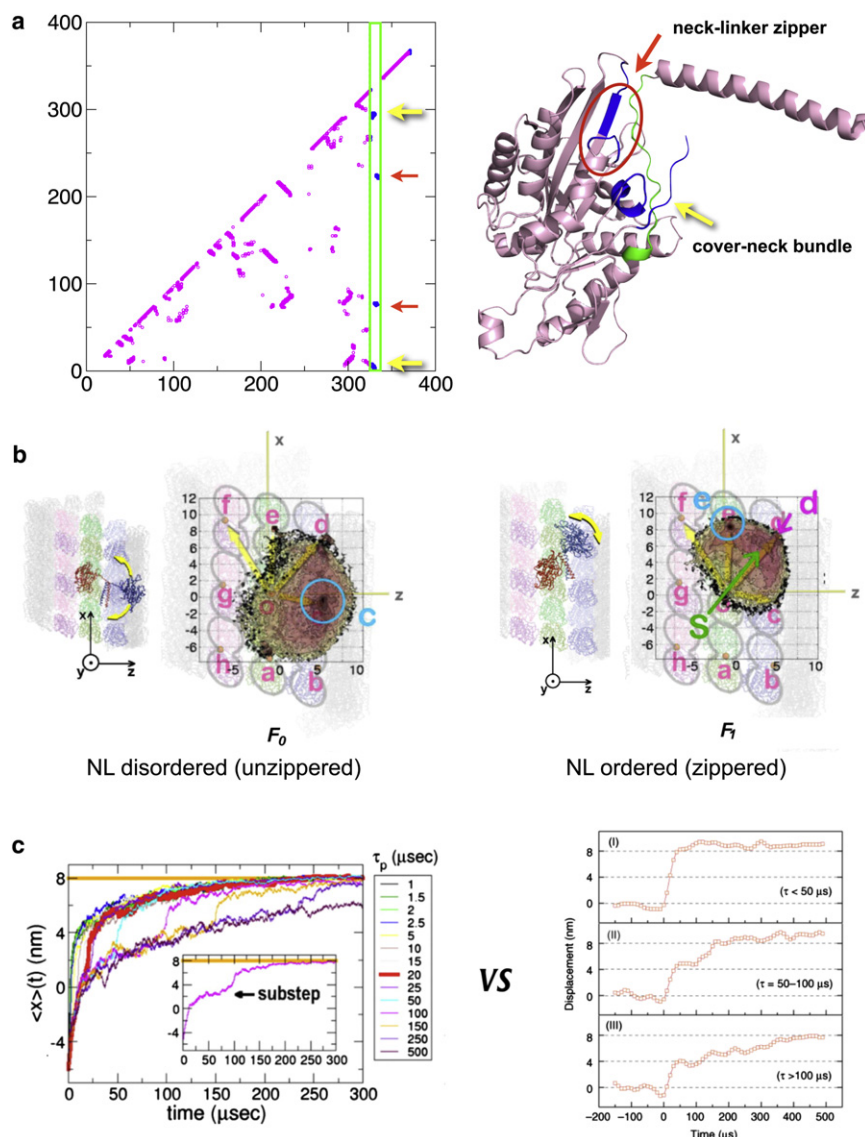
FIGURE 2 Stepping dynamics of kinesin. (*a*) Difference of contact maps calculated with ordered and disordered NL reveals the contacts involving the NL docking and cover-neck bundle. Red arrows indicate the NL zipper contacts on the contact map and in the kinesin structure. Yellow arrows show the location of cover-neck bundle, where the N-terminal part of NL is sandwiched between two chain segments (residues 2–8 and 289–296). (*b*) Potential of mean force of the tethered head on the MT surface computed for disordered (*left*) and ordered NL (*right*) of the MT-bound head. (*c*) The average time traces from the Brownian dynamics simulation of a quasiparticle with varying τ_P (*panel on the left*) are compared with the average time traces measured using optical tweezers by Yanagida and co-workers (*three panels on the right*) (27). In (27), the individual single molecule time traces were partitioned into three groups depending on the stepping time i), $t < 50$ μs, ii), 50 μs $< t < 100$ μs, iii), $t > 100$ μs) and averaged in each group. The panels on the right are adapted from (27).

kinesin cycle. Nevertheless, because the timescale associated with this motion (~ (10 –100) μsec) is transient compared with that of the entire cycle (> 10 ms), details of the dynamics has been elusive and under intensive debate (9,27,47,48). The simple looking jump from one binding site to another, in fact, contains many complicated dynamics at molecular level: i), The NL restrains the dynamics of the tethered head. ii), Depending on the NT state, the NL conformation is either in disordered or ordered state, which influences the range of space for the tethered head to explore. The disorder-order transition of the NL in the MT-bound head can rectify the diffusive motion of tethered head toward the next MT binding site. iii), MTs provide multiple binding sites for kinesins. Given the microscopic constraints and dynamics described previously, what is the dynamical or structural origin of substeps observed in some of the experiments (27,47)? To what portion of entire

stepping motion is contributed by the motion due to NL docking and diffusive search?

Probing the stepping dynamics at molecular detail is even now an extremely demanding task because of the limited spatial and temporal resolutions of the current instrumentation (9,27,47,48). Therefore, a molecular model is of great help to study this particular problem (14). Kinesin models of ordered and disordered NL, created by adjusting the strength of the NL native contacts (Fig. 2 *a*), were used to calculate the potentials of mean force and to visualize how the formation of NL zipper changes the search space for the tethered head. Under the disordered NL, the tethered head spans the broad area around the sideway binding site (*c* in Fig. 2 *b*), but cannot reach the next target binding site (*e* in Fig. 2 *b*). When the NL is in the docked state, the search space is confined preferentially to the forward direction relative to the MT-bound head, guiding the tethered head to the

target binding site. A theoretical consideration based on two competing timescales can be proposed; if the disorder-order NL docking transition is slower than the timescale associated with exploring the MT surface, so that the tethered head can fully explore the MT surface while the NL is still in the disordered state, then the sideway binding site (c in Fig. 2 b) can transiently trap the swinging tethered head; and consequently a substep emerges in the averaged time trace. The above scenario of sideway binding during the stepping can be simulated using the dynamics of a quasiparticle on a time-dependent free energy surface

$$F(\vec{r}, t)/k_{\mathrm{B}}T = -\log\left[\left(\frac{t}{\tau_p}\right) \times e^{-F_0(\vec{r})/k_{\mathrm{B}}T} + \left(1 - \frac{t}{\tau_p}\right) \times e^{-F_1(\vec{r})/k_{\mathrm{B}}T}\right]$$

for $t \leq \tau_p$ and $F(\vec{r}, t) = F_1(\vec{r})$ for $t > \tau_p$. This combines the potentials of mean force at the two extreme cases; $F_0(\vec{r})$ under disordered NL and $F_1(\vec{r})$ under ordered NL. Here, τ_p is a parameter for the duration of NL docking transition. For a quasiparticle representing the centroid of tethered head with a diffusion constant $D = 0.2\ \mu\mathrm{m}^2/\mathrm{s}$, the averaged time traces exhibit the signature of a substep when τ_p is greater than $\approx 20\ \mu\mathrm{s}$ (Fig. 2 c left), which is similar to the one observed by Yanagida and co-workers (27) (see Fig. 2 c right). Our theoretical study using a multiscale simulation method suggests that the ratio between the timescale of NL zipper dynamics and the exploration time on MT surface determines the detailed pattern of the stepping (14).

Interestingly, the recent experiment by Yildiz et al. (49) for wild-type kinesin using a quantum dot labeling displayed $\approx 13\%$ of 6-nm displacement, which is likely to be the signature of sideway steps to the neighboring protofilament. Given the longstanding debate on the existence of kinesin substep (9,27,47,48), reinvestigating kinesin time traces using an instrument with improved temporal and spatial resolution would be of great interest.

FACTORS DETERMINING MOTOR DIRECTIONALITY

Despite a remarkable similarity among the head domain structures from ≈ 50 different kinesins belonging to the same family, the functions of kinesins are diverse; kinesin-1 moves toward (+)-end, kinesin-14 (C-terminal motor) moves toward (−)-end, kinesin-3 (KIF1A) undergoes diffusive motion along MTs (50), and kinesin-13 quickly diffuses along MTs to reach the ends to depolymerize tubulins (51). Given the structures of a motor with varying NT states and motor track, what determines the directionality of the motor? Brownian ratchet models suggest three basic conditions for the unidirectional motion: i), asymmetric potential, ii), thermal fluctuation, and iii), athermal fluctuation (flashing ratchet or fluctuating potential) (52).

In kinesins, these three conditions are realized through the interplay of several factors. First, the interaction of kinesins in ADP-ADP state with MTs results in dissociation of an ADP from one of the two heads, breaking the symmetry of NT state of the two heads. Throughout the entire cycle, NT states remain asymmetric in the two motor heads. Second, kinesin motor domain binds MT in preferred direction, so that the NL in ordered state points toward the (+)-end of MTs. Third, as clearly demonstrated in Fig. 2 b, the ordered state of NL restrains the search space of swinging head toward the (+)-end direction. Finally, the irreversibility of ATP hydrolysis sets the arrow of time, breaking the time reversal symmetry.

Given the thermal and athermal (ATP-cycle) fluctuations that are provided as a basic driving force for the conformational change in biological enzymes, the directionality of a biological motor is determined by the structure and conformational dynamics and its specific interaction with cytoskeletal filaments and other proteins (53).

CONFORMATIONAL FLEXIBILITY: A STRATEGY TO AVOID HIGH FREE ENERGY BARRIERS

A stark difference in the dynamics of biological motors from that of macroscopic machines is that the intrinsic energy scale responsible for the biological assembly is comparable to the thermal energy (see also Supporting Material). It is well entrenched that free energy gaps between functional states of biomolecules are marginal (54), thus a biomolecule can easily adapt its conformation to environmental changes due to chemical transformation of molecular fuels and external tension. In addition, the flexibility of biomolecules makes their characteristic dynamics entirely different from that of a macroscopic system. For instance, binding between two partner molecules such as enzyme and substrate protein does not necessitate an absolute geometrical complementarity (55). As suggested by Koshland, (56) it is more likely for flexible biomolecules that interactions between biomolecules are realized through a mutual adaptation of the structures.

The mechanisms of partial unfolding/refolding and fly casting to avoid a large binding free energy barrier have been theoretically postulated (57–59) and experimentally implicated (60,61) in binding processes associated with protein-protein or DNA-protein interaction, and in proteins with an intrinsically disordered region (62). Our calculation suggests that kinesins also adopt this strategy to march along the MT by efficiently identifying the next MT binding site. Although the transient disruption of local structure may be difficult to detect, such dynamics could be important if free energy barrier associated with protein-protein recognition is too high. Indeed, the simulation of the binding process of our kinesin model on MTs showed that the partial disruption of the internal structure facilitates the binding dynamics of kinesin (14). The binding events monitored

by using the native contacts of the kinesin's MT-binding motifs (Q_p) and the interface contacts between the kinesin and MT (Q_{int}) show a transient decrease of Q_p value before binding (Fig. 3). The transient partial local unfolding and refolding help the kinesin bind the MTs by bypassing a high free energy barrier.

OUT-OF-PHASE HEAD-HEAD COORDINATION IN THE ENZYMATIC CYCLE

Although biomolecules generally fold to function, interaction with other molecules can restrain a part of molecular structure, deliberately suppressing its ability to fold. Such a strategy is found in the design principles of biological motors that consist of multiple domains. In particular, dimeric kinesin maintains the asymmetrical chemical state in two motor heads and accomplish processive steps along MTs.

For kinesins to maintain a high processivity, the enzymatic cycle of each head is kept out of phase. A quest to understanding the molecular origin of the head-head coordination has been pursued over the last decade. It has been surmised based on a series of experiments that the tension on NL is responsible for the out-of-phase coordination between the two motor domains. Nevertheless, it was not straightforwardly determined whether such coordination is realized due to the facilitated detachment of trailing head induced by forward tension (63) or due to the rearward tension-induced inhibition of ATP binding to the leading head (33,64). Remarkably, treating the MT surface as a geometrical constraint on which the kinesin dynamics occurs, our molecular simulation using a C_α-based coarse-grained model of kinesin suggests that, when both heads of kinesin are bound to the MT binding site as in ATP-ϕ or ADP·Pi-ϕ

states, the NL of the leading head that is stretched backward perturbs the catalytic site of the leading head away from its native-like configuration, whereas the catalytic site of trailing head remains intact (13). The internal tension (f_{int}) exerted through the NL, estimated using the extension of the NL calculated from the simulation (δx) and the force-extension relationship of a worm-like chain model ($f_{int} = k_B T/l_p \times [1/4(1 - \delta x/L)^2 - 1/4 + \delta x/L]$), is $8 - 15$ pN depending on the l_p value assigned (13). The structure-function relationship implies that the deformation of catalytic site results in the loss of ATP binding affinity to the catalytic site, thus inhibiting the premature binding of ATP. Such an ATP inhibition state is maintained as long as the two heads remain bound to MTs. The deformed leading head catalytic site is restored only after the P_i is released to change the trailing kinesin head from a strong to weak affinity state with respect to MTs. In addition to the inhibition of ATP binding, the disruption of the catalytic site in the leading head regulates the off-rate of ADP (k_{off}^{ADP}), which was also discussed by Uemura et al. (64). Note that $k_{off}^{ADP} = 75 - 100$ s^{-1} (30), 300 s^{-1} (65) in the leading head but $k_{off}^{ADP} = 1$ s^{-1} in the trailing head. The asymmetric strain-induced regulation mechanism (33,64), the molecular origin of the head-head coordination, and processivity unique to the kinesin-1, is the consequence of the interplay between several topological constraints imposed on kinesin/MT complex structure. By explicitly showing the perturbed configuration at the catalytic site of the leading head (Fig. 4), our computational study using the simple structure-based model supports the experimental proposal of the rearward strain regulation mechanism between the two motor heads (13,33,49,64,66).

DIAGRAM OF INTERNAL TENSION VERSUS EXTENSION CURVE FOR THE NECK LINKER

In contrast to the thermodynamic conditions imposed on macroscopic engines, molecular motors operate under isothermal and highly dissipative environments; thus, a thermodynamic cycle with two distinct isotherms as in the Carnot engine is not applicable for biological motors (Fig. S1). Instead, conformational changes of internal structure can be linked to the thermodynamic cycle. As a simple example, the thermodynamics of the optomechanical coupling in polyazopeptide (67) is best described in terms of two thermodynamically conjugate variables, force (f) and extension (x) (Fig. 5 a). Photon absorption/emission transforms the polymeric property of polyazopeptide, the persistence length (l_p) and contour length (L_c), via $cis \leftrightarrow trans$ conformational change. The two distinct force-extension curves with different l_p and L_c, corresponding to the distinct conformational states of polyazopeptide, are analogous to the two isotherms in the Carnot cycle. The area enclosed by the optomechanical cycle is the maximal mechanical work that the polymer engine can extract from the photon energy when the polymer is stretched and relaxed quasistatically.
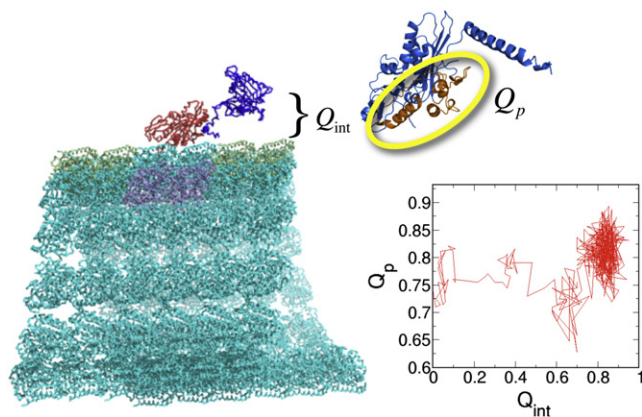

FIGURE 3 Facilitation of kinesin binding to MTs through partial unfolding and refolding of MT-binding motifs. Binding process is monitored using the fraction of native contacts within the MT-binding motifs made of $\alpha 4$, $\alpha 5$, $\alpha 6$, $L12$, and $\beta 5$ (Q_p) and the fraction of interfacial contacts between kinesin and MT binding site (Q_{int}). The inset shows an exemplary trajectory exhibiting partial local unfolding and refolding of MT-binding motifs before the binding.
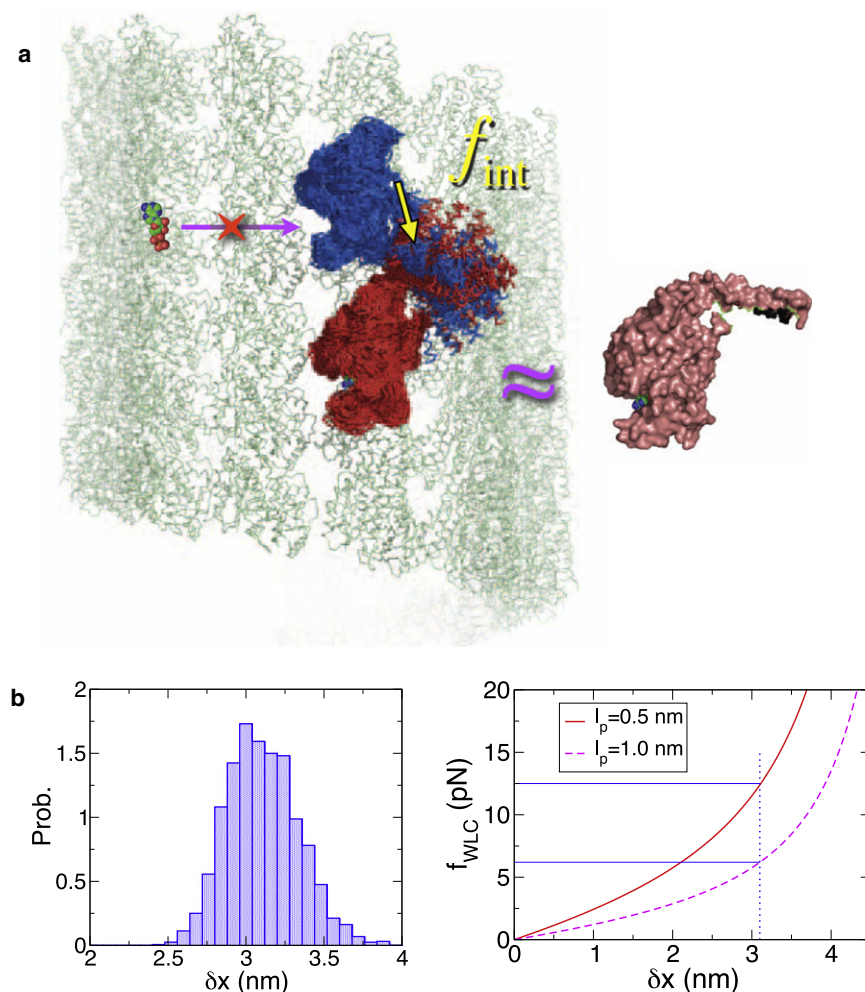
FIGURE 4 Internal tension regulated inhibition of ATP binding to the leading kinesin head. (a) For the two head-bound kinesin, the internal tension (f_{int}) built on the NL of the leading head disrupts the catalytic site and inhibits the premature binding of ATP, whereas the trailing head configuration is close to the native state, which is shown on the right for comparison. C_α-root mean-square deviation of head domain excluding $\alpha 6$ helix (residues 2–315) is 1.8 Å for trailing head and 3.8 Å for leading head. (b) f_{int} value can be estimated by using force-extension relation of the worm-like chain model. The extension of the NL in the leading head (δx) is $\approx$ 3.1 $\pm$ 0.8 nm (distribution on the left panel). When $L_c = 15$ aa $\times$ 0.38 nm/aa $\approx$ 5.7 nm and $l_p = 0.5 - 1.0$ nm with $\delta x = 3.1$ nm are used, one can estimate the internal tension, $f_{int} \approx 7.5 - 12.5$ pN (right panel).

Biological machines adopt a similar strategy as the polyazopeptide by changing molecular conformations in response to the interactions with molecular fuels. In analogy to polyazopeptide whose mechanical property and conformational change are used to generate work, it is essential to identify relevant structural elements, responsible for internal mechanics, from its complicated architecture, to understand the work generating mechanism of each biological motor.

For kinesin, as suggested in the previous sections, the NL is one of the key structural elements responsible for both the stepping dynamics and head-head regulation. Along the biochemical cycle, the change in motor head affinity to MTs as well as the disorder-order transition of the NL alters the polymer property of NL. By assuming that NL, a 15 amino acid polypeptide segment, is well described using a worm-like chain model (see, however, (68)), we propose a diagram in Fig. 5 b that depicts the magnitude of an internal tension (f_{int}) built on one of the NLs (NL of red motor head) versus its extension (δx) with its direction ($\delta x > 0$ for forward and $\delta x < 0$ for backward extension) for the full cycle. The diagram of thermodynamic cycle, built by

tracking the state of NL along the biochemical cycle of kinesin, provides an integrated view of how the extension/release and conformational change of NL lead to generate work and regulate the head-head coordination.

In (i)→(ii), the NL changes both the length and direction upon docking transition. In this step the residue 326 binds $\beta 10$ to form a β-sheet, leaving only two residues at the C-terminal of the NL. As a result, the contour length of the NL (L_c) decreases from $L_c \approx 5.7$ to ≈ 1.0 nm. The $L_c \approx 1.0$ nm is maintained until Pi is released from the trailing (red) head at the state (v). After an ADP released at (ii)→(iii), the leading (blue) head strongly binds the MT. In (iii)→(iv)→(v), Pi release from the trailing head is followed by the order-disorder transition in the NL, which restores the contour length into $L_c = 5.7$ nm. If (v)→(vi) step were to occur quasistatically, force mechanics of the NL would follow the line of the force-extension curve. Along (vi)→(vii)→(viii)→(i), the value of L_c does not change but because the binding affinity of the trailing (blue) head is altered, the f_{int} built on the NL is expected to vary.
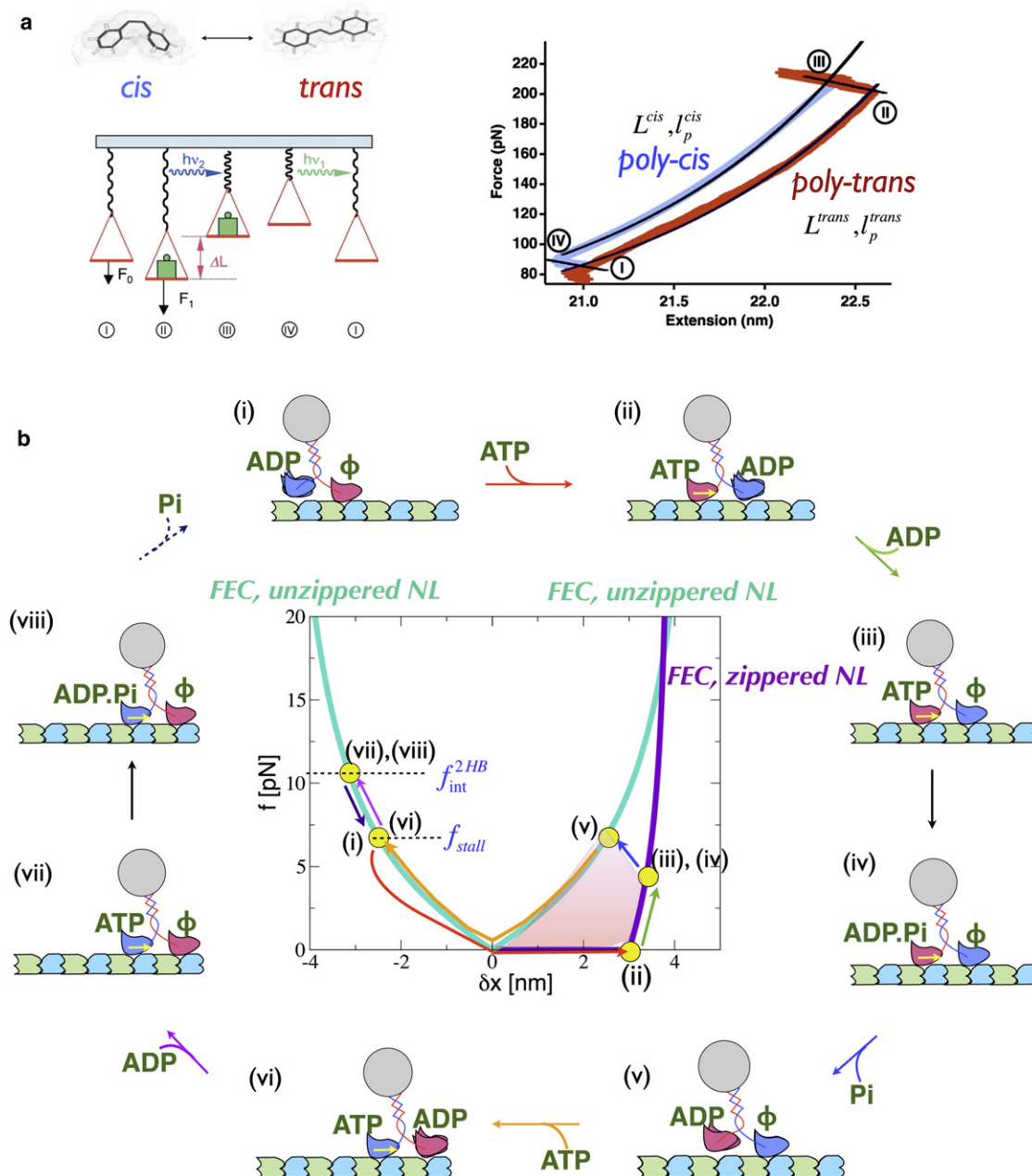
FIGURE 5 (*a*) Molecular motor devised by using optomechanical cycle of polyazopeptide that undergoes *cis* ↔ *trans* transition upon photon absorption/ emission. The figure is adapted from (67). (*b*) The mechanochemical cycle of kinesins and the force versus extension curves (FECs) for the NL of red motor domain. There are three FECs; two for the unzipped NL (*cyan*) and one for the zipped NL (*purple*). Each stage of kinesin cycle is marked with the yellow circles on the FECs indexed from (i) to (viii).

The thermodynamic cycle of kinesin by focusing on the force extension property of one of the NLs (Fig. 5 *b*) makes a few interesting points. First, the f_{int} would be greatest when the two motor heads are simultaneously bound to the MT. By assuming $l_p = 0.6$ nm for the NL, the f_{int} for the two-head bound (2HB) state (see the section discussing the nature of ATP-wait state in Supporting Material) is expected to be $f_{int}^{2HB} \approx 11$ pN. It is of particular note that the estimated value of $f_{int}^{2HB} \approx 11$ pN should not be confused

with the value of force ($f_{stall} \approx 6 - 7$ pN) externally applied through the coiled-coil stalk that can stall the kinesin motion (49). While f_{stall} interferes with the step (i) → (ii) or (v) → (vi) by preventing the NL zipper process, the f_{int}^{2HB} on the NL is used to regulate the head-head coordination. In addition, the diagram suggests that $f_{int}^{2HB} > f_{stall}$. Second, the diagram of thermodynamic cycle succinctly indicates the origin of symmetry breaking, which gives rise to the motor direction-ality. The finite area enclosed by force extension curves is

formed along the process from (i) to (vi) while the process involving (vi)→(vii)→(viii)→(i) creates no work. Among the series of different kinesin configurations, the work generating conformational change of NL occurs while the motor head is mostly in the trailing position ($\delta x > 0$) and its configuration is sequentially altered from ATP state to ADP state (see the red head in Fig. 5 b). Third, during the process of conformational change in red head spanning the half-cycle, the partner (blue) head is mostly in NT free state, waiting for the enzymatic cycle of the red head to be completed. It is noteworthy that although the process (vi)→(vii)→(viii)→(i) creates no work, during which the NL of the red head points the rearward direction ($\delta x < 0$), the f_{int} whose value changes between f_{stall} and f_{int}^{2HB} is used to inhibit the ATP binding, which recapitulates the origin of head-head coordination.

The thermodynamic cycle for the NL of kinesin (Fig. 5 b), similar to the optomechanical cycle of polyazopeptide (Fig. 5 a), highlights the NL as a key structural element of work generation and regulation in kinesin dynamics.

CONCLUDING REMARKS

In this work, using coarse-grained molecular simulations and theoretical considerations based on the theories of protein folding and polymer dynamics, we presented our perspective on how the kinesin, under significant thermal fluctuation, orchestrates its structure, conformational dynamics, and interaction with NT and MTs to constitute the characteristic biochemical cycle. We adopted into our coarse-grained model the hypothesis of structure-function relationship (69) from the study of protein function and its extension to protein-protein and protein-ligand interactions, and tried to address several key issues in the kinesin dynamics. Although a series of rate constants that constitute the enzymatic cycle may allow us to formally explain the behavior of kinesin motor as a function of external force or concentration of ATP (70), the chemical specificity of the motor itself, encoded in the microscopic rate constant and affinity to the MT, is determined by the structural details at each stage of the cycle. It is impressive to see a number of recent experimental efforts to engineer the chemical specificity of kinesin by altering various structural elements, which includes changing the length of NL (49,71,72), mutating the amino acid at the neck region (73), and removing the negatively charged C-terminal region of tubulin (E-hook) (74,75). The mechanical notions we tried to employ with our computational model in this work such as stress, strain, deformation, tension, persistence length should be useful to clarify why the microscopic rate constant or affinity has that particular value and provide a better idea to understand and engineer the dynamics of biological motors.

Finally, the notion of motor efficiency is worth mentioning. Although the literature often discusses the unusually high thermodynamic efficiency of biological motors (76,77), the thermodynamic efficiency itself may not be such a relevant measure to understand the principles of biological motors in the cell where the amount of molecular fuels are buffered by the cellular metabolism. Depending on the functional goal of a biological motor, the optimization criteria may vary (78). Analysis of the energy balance of kinesins (35) indicates that at the physiological condition, 60% of the free energy stored in ATP is expended upon ATP binding to induce the conformational changes directly linked to the stepping dynamics; the remaining 40% of free energy due to the sequence of processes followed by ATP binding is partitioned into several microscopic steps that do not produce any work (36). As discussed throughout the work, the nonwork producing steps, depicted with purple arrows in Fig. 1 or the processes corresponding to (vi)→(vii)→(viii)→(i) in Fig. 5 b, are responsible for regulating the MT affinity of kinesin motor domain, the configurational state of NL, and the NT state of partner head through head-head coordination. Similar to the concept of kinetic proofreading to increase the fidelity of biological processes (37), the series of nonwork producing steps, which otherwise appear to be aimless side reactions, are essential for kinesins to have the persistent motor function. To regulate the molecular configurations under excessive thermal noise, biological motors reserve a substantial amount of free energy. Understanding the mechanism of allosteric regulation at the microscopic level would be one of the important topics to explore in the study of biological motors.

SUPPORTING MATERIAL

REFERENCES

1. Feynman, R. P. 1961. Miniaturization. Reinhold, New York.

2. Alberts, B. 1998. The cell as a collection of protein machines: preparing the next generation of molecular biologists. *Cell.* 92:291–294.

3. Hirokawa, N. 1998. Kinesin and dynein superfamily proteins and the mechanism of organelle transport. *Science.* 279:519–526.

4. Vale, R. D. 2003. The molecular motor toolbox for intracellular transport. *Cell.* 112:467–480.

5. Harms, J., F. Schluenzen, …, A. Yonath. 2001. High resolution structure of the large ribosomal subunit from a mesophilic eubacterium. *Cell.* 107:679–688.

6. Nissen, P., J. Hansen, …, T. A. Steitz. 2000. The structural basis of ribosome activity in peptide bond synthesis. *Science.* 289:920–930.

7. Alberts, B., A. Johnson, …, P. Walter. 2008. Molecular Biology of the Cell, 5th ed. Garland Science, New York.

8. Alberts, B., and R. Miake-Lye. 1992. Unscrambling the puzzle of biological machines: the importance of the details. *Cell.* 68:415–420.

9. Block, S. M. 2007. Kinesin motor mechanics: binding, stepping, tracking, gating, and limping. *Biophys. J.* 92:2986–2995.

10. Greenleaf, W. J., M. T. Woodside, and S. M. Block. 2007. High-resolution, single-molecule measurements of biomolecular motion. *Annu. Rev. Biophys. Biomol. Struct.* 36:171–190.

11. Koga, N., and S. Takada. 2006. Folding-based molecular simulations reveal mechanisms of the rotary motor F_1-ATPase. *Proc. Natl. Acad. Sci. USA.* 103:5367–5372.

12. Hyeon, C., G. H. Lorimer, and D. Thirumalai. 2006. Dynamics of allosteric transitions in GroEL. *Proc. Natl. Acad. Sci. USA.* 103:18939–18944.

13. Hyeon, C., and J. N. Onuchic. 2007. Internal strain regulates the nucleotide binding site of the kinesin leading head. *Proc. Natl. Acad. Sci. USA.* 104:2175–2180.

14. Hyeon, C., and J. N. Onuchic. 2007. Mechanical control of the directional stepping dynamics of the kinesin motor. *Proc. Natl. Acad. Sci. USA.* 104:17382–17387.

15. Chen, J., S. A. Darst, and D. Thirumalai. 2010. Promoter melting triggered by bacterial RNA polymerase occurs in three steps. *Proc. Natl. Acad. Sci. USA.* 107:12523–12528.

16. Tehver, R., and D. Thirumalai. 2010. Rigor to post-rigor transition in myosin V: link between the dynamics and the supporting architecture. *Structure.* 18:471–481.

17. Takano, M., T. P. Terada, and M. Sasai. 2010. Unidirectional Brownian motion observed in an in silico single molecule experiment of an actomyosin motor. *Proc. Natl. Acad. Sci. USA.* 107:7769–7774.

18. Kravats, A., M. Jayasinghe, and G. Stan. 2011. Unfolding and translocation pathway of substrate protein controlled by structure in repetitive allosteric cycles of the ClpY ATPase. *Proc. Natl. Acad. Sci. USA.* 108:2234–2239.

19. Anderson, P. W. 1997. Basic Notions of Condensed Matter Physics. Westview Press, Boulder, CO.

20. Hyeon, C., and D. Thirumalai. 2011. Capturing the essence of folding and functions of biomolecules using coarse-grained models. *Nat Commun.* 2:487.

21. Onuchic, J. N., and P. G. Wolynes. 2004. Theory of protein folding. *Curr. Opin. Struct. Biol.* 14:70–75.

22. Shakhnovich, E. 2006. Protein folding thermodynamics and dynamics: where physics, chemistry, and biology meet. *Chem. Rev.* 106:1559–1588.

23. Dill, K. A., S. B. Ozkan, …, T. R. Weikl. 2008. The protein folding problem. *Annu. Rev. Biophys.* 37:289–316.

24. Thirumalai, D., E. P. O'Brien, …, C. Hyeon. 2010. Theoretical perspectives on protein folding. *Annu. Rev. Biophys.* 39:159–183.

25. de Gennes, P. G. 1979. Scaling Concepts in Polymer Physics. Cornell University Press, Ithaca, New York.

26. Asbury, C. L., A. N. Fehr, and S. M. Block. 2003. Kinesin moves by an asymmetric hand-over-hand mechanism. *Science.* 302:2130–2134.

27. Nishiyama, M., E. Muto, Y. Inoue, T. Yanagida, and H. Higuchi. 2001. Substeps within the 8-nm step of the ATPase cycle of single kinesin molecules. *Nat. Cell Biol.* 3:425–428.

28. Yildiz, A., M. Tomishige, …, P. R. Selvin. 2004. Kinesin walks hand-over-hand. *Science.* 303:676–678.

29. Sindelar, C. V., and K. H. Downing. 2010. An atomic-level mechanism for activation of the kinesin molecular motors. *Proc. Natl. Acad. Sci. USA.* 107:4111–4116.

30. Ma, Y. Z., and E. W. Taylor. 1997. Interacting head mechanism of microtubule-kinesin ATPase. *J. Biol. Chem.* 272:724–730.

31. Cross, R. A., I. Crevel, …, L. A. Amos. 2000. The conformational cycle of kinesin. *Philos. Trans. R. Soc. Lond. B Biol. Sci.* 355:459–464.

32. Xing, J., W. Wriggers, …, S. S. Rosenfeld. 2000. Kinesin has three nucleotide-dependent conformations. Implications for strain-dependent release. *J. Biol. Chem.* 275:35413–35423.

33. Guydosh, N. R., and S. M. Block. 2006. Backsteps induced by nucleotide analogs suggest the front head of kinesin is gated by strain. *Proc. Natl. Acad. Sci. USA.* 103:8054–8059.

34. Gilbert, S. P., and K. A. Johnson. 1994. Pre-steady-state kinetics of the microtubule-kinesin ATPase. *Biochemistry.* 33:1951–1960.

35. Hackney, D. D. 2005. The tethered motor domain of a kinesin-microtubule complex catalyzes reversible synthesis of bound ATP. *Proc. Natl. Acad. Sci. USA.* 102:18338–18343.

36. Hyeon, C., S. Klumpp, and J. N. Onuchic. 2009. Kinesin's backsteps under mechanical load. *Phys. Chem. Chem. Phys.* 11:4899–4910.

37. Hopfield, J. J. 1974. Kinetic proofreading: a new mechanism for reducing errors in biosynthetic processes requiring high specificity. *Proc. Natl. Acad. Sci. USA.* 71:4135–4139.

38. Hyeon, C., P. A. Jennings, …, J. N. Onuchic. 2009. Ligand-induced global transitions in the catalytic domain of protein kinase A. *Proc. Natl. Acad. Sci. USA.* 106:3023–3028.

39. Parke, C. L., E. J. Wojcik, …, D. K. Worthylake. 2010. ATP hydrolysis in Eg5 kinesin involves a catalytic two-water mechanism. *J. Biol. Chem.* 285:5859–5867.

40. Rice, S., A. W. Lin, …, R. D. Vale. 1999. A structural change in the kinesin motor protein that drives motility. *Nature.* 402:778–784.

41. Sindelar, C. V., M. J. Budny, …, R. Cooke. 2002. Two conformations in the human kinesin power stroke defined by x-ray crystallography and EPR spectroscopy. *Nat. Struct. Biol.* 9:844–848.

42. Rice, S., Y. Cui, …, R. Cooke. 2003. Thermodynamic properties of the kinesin neck-region docking to the catalytic core. *Biophys. J.* 84:1844–1854.

43. Hwang, W., M. J. Lang, and M. Karplus. 2008. Force generation in kinesin hinges on cover-neck bundle formation. *Structure.* 16:62–71.

44. Khalil, A. S., D. C. Appleyard, …, M. J. Lang. 2008. Kinesin's cover-neck bundle folds forward to generate force. *Proc. Natl. Acad. Sci. USA.* 105:19247–19252.

45. Czövek, A., G. J. Szöllosi, and I. Derényi. 2011. Neck-linker docking coordinates the kinetics of kinesin's heads. *Biophys. J.* 100:1729–1736.

46. Oosawa, F. 2000. The loose coupling mechanism in molecular machines of living cells. *Genes Cells.* 5:9–16.

47. Coppin, C. M., J. T. Finer, …, R. D. Vale. 1996. Detection of sub-8-nm movements of kinesin by high-resolution optical-trap microscopy. *Proc. Natl. Acad. Sci. USA.* 93:1913–1917.

48. Carter, N. J., and R. A. Cross. 2005. Mechanics of the kinesin step. *Nature.* 435:308–312.

49. Yildiz, A., M. Tomishige, …, R. D. Vale. 2008. Intramolecular strain coordinates kinesin stepping behavior along microtubules. *Cell.* 134:1030–1041.

50. Nitta, R., M. Kikkawa, …, N. Hirokawa. 2004. KIF1A alternately uses two loops to bind microtubules. *Science.* 305:678–683.

51. Helenius, J., G. Brouhard, …, J. Howard. 2006. The depolymerizing kinesin MCAK uses lattice diffusion to rapidly target microtubule ends. *Nature.* 441:115–119.

52. Astumian, R. D. 1997. Thermodynamics and kinetics of a Brownian motor. *Science.* 276:917–922.

53. Roostalu, J., C. Hentrich, …, T. Surrey. 2011. Directional switching of the kinesin Cin8 through motor coupling. *Science.* 332:94–99.

54. Branden, C., and J. Tooze. 1991. Introduction to Protein Structure. Garland Publishing, New York.

55. Fischer, E. 1894. Einfluss der configuration auf die wirkung der enzyme. *Ber. Dt. Chem. Biol.* 27:2985–2993.

56. Koshland, D. E. 1958. Application of a Theory of Enzyme Specificity to Protein Synthesis. *Proc. Natl. Acad. Sci. USA.* 44:98–104.

57. Shoemaker, B. A., J. J. Portman, and P. G. Wolynes. 2000. Speeding molecular recognition by using the folding funnel: the fly-casting mechanism. *Proc. Natl. Acad. Sci. USA.* 97:8868–8873.

58. Miyashita, O., J. N. Onuchic, and P. G. Wolynes. 2003. Nonlinear elasticity, proteinquakes, and the energy landscapes of functional transitions in proteins. *Proc. Natl. Acad. Sci. USA.* 100:12570–12575.

59. Levy, Y., S. S. Cho, …, P. G. Wolynes. 2005. A survey of flexible protein binding mechanisms and their transition states using native topology based energy landscapes. *J. Mol. Biol.* 346:1121–1145.

60. Spolar, R. S., and M. T. Record, Jr. 1994. Coupling of local folding to site-specific binding of proteins to DNA. *Science.* 263:777–784.

61. Dyson, H. J., and P. E. Wright. 2005. Intrinsically unstructured proteins and their functions. *Nat. Rev. Mol. Cell Biol.* 6:197–208.

62. Dunker, A. K., C. J. Brown, …, Z. Obradović. 2002. Intrinsic disorder and protein function. *Biochemistry.* 41:6573–6582.

63. Hancock, W. O., and J. Howard. 1999. Kinesin's processivity results from mechanical and chemical coordination between the ATP hydrolysis cycles of the two motor domains. *Proc. Natl. Acad. Sci. USA.* 96:13147–13152.

64. Uemura, S., and S. Ishiwata. 2003. Loading direction regulates the affinity of ADP for kinesin. *Nat. Struct. Biol.* 10:308–311.

65. Moyer, M. L., S. P. Gilbert, and K. A. Johnson. 1998. Pathway of ATP hydrolysis by monomeric and dimeric kinesin. *Biochemistry.* 37:800–813.

66. Miyazono, Y., M. Hayashi, …, H. Tadakuma. 2010. Strain through the neck linker ensures processive runs: a DNA-kinesin hybrid nanomachine study. *EMBO J.* 29:93–106.

67. Hugel, T., N. B. Holland, …, H. E. Gaub. 2002. Single-molecule optomechanical cycle. *Science.* 296:1103–1106.

68. Kutys, M. L., J. Fricks, and W. O. Hancock. 2010. Monte Carlo analysis of neck linker extension in kinesin molecular motors. *PLOS Comput. Biol.* 6:e1000980.

69. Bryngelson, J. D., J. N. Onuchic, …, P. G. Wolynes. 1995. Funnels, pathways, and the energy landscape of protein folding: a synthesis. *Proteins.* 21:167–195.

70. Astumian, R. D. 2010. Thermodynamics and kinetics of molecular motors. *Biophys. J.* 98:2401–2409.

71. Hackney, D. D., M. F. Stock, …, R. A. Patterson. 2003. Modulation of kinesin half-site ADP release and kinetic processivity by a spacer between the head groups. *Biochemistry.* 42:12011–12018.

72. Clancy, B. E., W. M. Behnke-Parks, …, S. M. Block. 2011. A universal pathway for kinesin stepping. *Nat. Struct. Mol. Biol.* 18:1020–1027.

73. Endow, S. A., and H. Higuchi. 2000. A mutant of the motor protein kinesin that moves in both directions on microtubules. *Nature.* 406:913–916.

74. Okada, Y., and N. Hirokawa. 2000. Mechanism of the single-headed processivity: diffusional anchoring between the K-loop of kinesin and the C terminus of tubulin. *Proc. Natl. Acad. Sci. USA.* 97:640–645.

75. Lakämper, S., and E. Meyhöfer. 2005. The E-hook of tubulin interacts with kinesin's head to increase processivity and speed. *Biophys. J.* 89:3223–3234.

76. Oster, G., and H. Wang. 2000. Why is the mechanical efficiency of $F_{(1)}$-ATPase so high? *J. Bioenerg. Biomembr.* 32:459–469.

77. Kinosita, Jr., K., R. Yasuda, …, K. Adachi. 2000. A rotary molecular motor that can work at near 100% efficiency. *Philos. Trans. R. Soc. Lond. B Biol. Sci.* 355:473–489.

78. Derényi, I., M. Bier, and R. D. Astumian. 1999. Generalized efficiency and its application to microscopic engines. *Phys. Rev. Lett.* 83:903–906.